Line shape of $\psi(3770)$ in $e^+e^- \to D\bar{D}$

N. N. Achasov [a]*, G. N. Shestakov [a]†

[a] *Laboratory of Theoretical Physics, S.L. Sobolev Institute for Mathematics, SD RAN, 630090 Novosibirsk, Russia*

Abstract

Interference phenomena observed in the $\psi(3770)$ resonance region in the reactions $e^+e^- \to D\bar{D}$ are analyzed. To avoid ambiguities in the determination of the $\psi(3770)$ resonance parameters, when analyzing data between the $D\bar{D}$ and $D\bar{D}\pi$ thresholds, the amplitudes satisfying the elastic unitarity requirement should be used. In the lack of information on the P-wave of $D\bar{D}$ elastic scattering, the $\psi(3770)$ parameters, determined by fitting the $e^+e^- \to D\bar{D}$ data, can essentially depend on the model used for the total contribution of the resonance and background. The selection of the models can be toughened by comparing their predictions with the relevant data on the shape of the $\psi(3770)$ peak in the non-$D\bar{D}$ channels $e^+e^- \to \gamma\chi_{c0}$, $J/\psi\eta$, $\phi\eta$, etc.

1. Introduction

The resonance $\psi(3770)$ was investigated in the reactions $e^+e^- \to D\bar{D}$ by the MARK-I [1], DELCO [2], MARK-II [3], BES [4, 5, 6], CLEO [7], BABAR [8], Belle [9], and KEDR [10, 11, 12] Collaborations. With increasing accuracy of measurements, there appeared indications on an unusual shape of the $\psi(3770)$ peak, i.e., on possible interference phenomena in its region [5, 6, 8, 9, 10, 11, 12, 13, 14]. It was also clear that the $\psi(3770)$ dose not have any other significant decay modes except decays to $D\bar{D}$, i.e., that it is an almost elastic resonance [15, 16].

Recently, the KEDR Collaboration noted [10, 11, 12] that the parameters of the $\psi(3770)$ resonance become distinctly different from those quoted by the Particle Data Group (PDG) in the preceding reviews (see, for example, Ref. [15]) if the data analysis takes into account the interference between the $\psi(3770)$ production amplitude and the nonresonant $D\bar{D}$ production one. In Refs. [11, 12], two very different solutions for the interfering resonance and background amplitudes were obtained (see also [16, 17]). These solutions lead to the same energy dependence of the cross section and are indistinguishable by the χ^2 criterion.

CLEO-c has now accumulated about 818 pb^{-1} [18] and BES III about 2.9 fb^{-1} [19] integrated luminosity on the $\psi(3770)$ peak for open charm physics investigations. Therefore, from CLEO-c and BES III, one can also expect new data with very high statistics on the shape of the $\psi(3770)$ resonance. In this regard, we believe it is timely to discuss some dangers which are hidden in the commonly used schemes for the description of the $\psi(3770)$ peak.

2. The $\psi(3770)$ in $e^+e^- \to D\bar{D}$

Figure 1 shows the data for the sum of the $e^+e^- \to D^0\bar{D}^0$ and $e^+e^- \to D^+D^-$ reaction cross sections in the $\psi(3770)$ region, $\sigma(e^+e^- \to D\bar{D})$, obtained by BES [5], CLEO [7], BABAR [8], and Belle [9]. In most experimental works, the $e^+e^- \to D\bar{D}$ cross section caused by the $\psi(3770)$ resonance production was described with minor modifications by the following formula (below, for short $\psi(3770)$ is also denoted as ψ''):

$$\sigma^{D\bar{D}}_{\psi''} = \frac{12\pi\Gamma_{\psi''e^+e^-}\Gamma_{\psi''D\bar{D}}(s)}{(m^2_{\psi''} - s)^2 + m^2_{\psi''}\Gamma^{tot\,2}_{\psi''}(s)} \quad \text{and} \quad \Gamma_{\psi''D\bar{D}}(s) = \frac{G^2_{\psi''}p^3_0(s)}{1 + r^2p^2_0(s)} + \frac{G^2_{\psi''}p^3_+(s)}{1 + r^2p^2_+(s)}, \qquad (1)$$

* **e-mail**: achasov@math.nsc.ru

† **e-mail**: shestako@math.nsc.ru

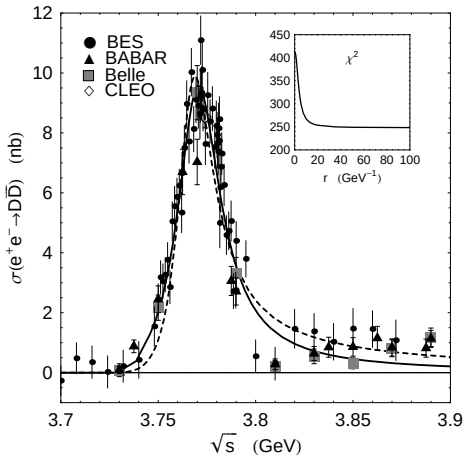

Figure 1: The data for $\sigma(e^+e^-\to D\bar{D})$ are from BES [5], CLEO [7], BABAR [8], and Belle [9]. The fits using Eqs. (1) illustrate the $\psi(3770)$ resonance shape dependence on the parameter r.

where $\sqrt{s}$ is the $D\bar{D}$ invariant mass, $p_{0,+}(s)=\sqrt{s/4-m^2_{D^{0,+}}}$, r the $D\bar{D}$ interaction radius, and $G_{\psi''}$ the $\psi''D\bar{D}$ coupling constant. Because the $\psi''\to D\bar{D}$ decay is dominant [16], we put $\Gamma^{tot}_{\psi''}(s)=\Gamma_{\psi''D\bar{D}}(s)$.

The dashed and solid curves in Fig. 1 show the fits to the data with the use of Eqs. (1) at $r=0$ and 100 GeV^{-1}, respectively. In the inset in this figure, the χ^2 quantity is shown as a function of r. As is seen from Fig. 1, a dip near 3.81 GeV cannot be explained by varying r. The obtained very unsatisfactory χ^2 values (for the dashed and solid curves in Fig. 1 $\chi^2\approx 413$ and 248, respectively) are due to both notable differences between the data from different groups and the existence of the dip (for the solid curve in Fig. 1, the points at $\sqrt{s}=3.8$ and 3.81 GeV yield $\chi^2\approx 81$). Thus, the current data on the $e^+e^-\to D\bar{D}$ in the ψ'' region are hard to describe with the help of a single ψ'' resonance contribution. In order to qualitatively improve the data description, in particular, to explain a dip near 3.81 GeV, it is necessary to take into account the interference between the resonant and nonresonant $D\bar{D}$ production.

3. The D meson electromagnetic form factor

• **Unitarity requirement.** In constructing the model describing the process $e^+e^-\to D\bar{D}$, one must keep in mind that we investigate above all the D meson isoscalar electromagnetic form factor, the phase of which in the elastic region is completely fixed by the unitarity condition (or the Watson theorem of final-state interaction). Experiment clearly indicates that we deal with the resonant scattering of D mesons. Really, there is the ψ'' resonance between the $D\bar{D}$ and $D\bar{D}^*$ thresholds ($2m_D\approx 3.739$ GeV and $m_D+m_{D^*}\approx 3.872$ GeV), which in a good approximation can be considered as an elastic one [16]. Usually, such scattering is described as resonance scattering with an elastic background [20], i.e., the corresponding $D\bar{D}$ scattering amplitude T^I_J with the isospin $I=0$ and spin $J=1$ is given by

$$T^0_1=e^{i\delta^0_1}\sin\delta^0_1=(e^{2i\delta_{bg}}-1)/(2i)+e^{2i\delta_{bg}}T_{res}\,, \qquad (2)$$

were $\delta^0_1=\delta_{bg}+\delta_{res}$ is the scattering phase, δ_{bg} is the elastic background phase, and δ_{res} is the phase of the resonance amplitude T_{res} Then, according to the unitarity condition $\mathrm{Im}F^0_D=F^0_D\,T^{0*}_1$, the D meson isoscalar form factor F^0_D has the form in the elastic region

$$F^0_D=e^{i\delta^0_1}G^0_D=e^{i(\delta_{bg}+\delta_{res})}G^0_D\,, \qquad (3)$$

where G^0_D is the real function of energy. A similar representation of the amplitude $e^+e^-\to D\bar{D}$ used for the data description guarantees the unitarity requirement on the model level. The sum

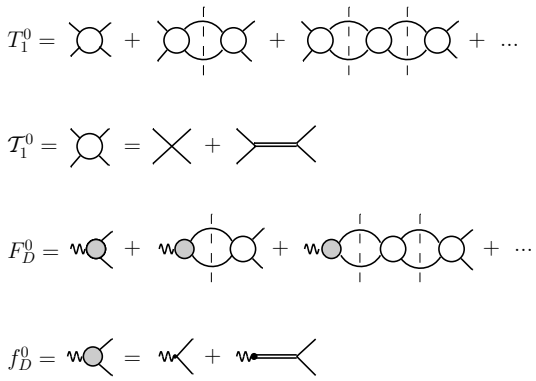

Figure 2: The graphical representation of the $D\bar{D}$ scattering amplitude T_1^0 and the D meson form factor F_D^0. The vertical dashed lines show that the D and $\bar{D}$ mesons in the loops are on the mass shell.

of the $e^+e^- \to D^0\bar{D}^0$ and $e^+e^- \to D^+D^-$ reaction cross sections is given by

$$\sigma^{D\bar{D}}(s) = \frac{8\pi\alpha^2}{3s^2}\left|F_D^0(s)\right|^2 \nu(s) \quad (\text{where} \;\; \nu(s) = (p_0^3(s) + p_+^3(s))/\sqrt{s}\,). \tag{4}$$

• **A simplest model for F_D^0: Resonance plus background.** To understand how the form factor and strong amplitude can be constructed to satisfy the unitarity requirement, the easiest way to use the field-theory model shown in Fig. 2 and write

$$T_1^0(s) = \frac{\mathcal{T}_1^0(s)}{1 - i\mathcal{T}_1^0(s)}\,, \;\; \mathcal{T}_1^0(s) = \nu(s)\, t_1^0(s)\,, \;\; t_1^0(s) = \lambda + \frac{1}{6\pi}\frac{g^2_{\psi'' D\bar{D}}}{m^2_{\psi''} - s}\,, \tag{5}$$

$$F_D^0(s) = \frac{f_D^0(s)}{1 - i\mathcal{T}_1^0(s)}\,, \quad f_D^0(s) = \lambda_\gamma + \frac{g_{\psi''\gamma} g_{\psi'' D\bar{D}}}{m^2_{\psi''} - s}\,. \tag{6}$$

Graphically, the amplitude $T_1^0(s)$ and the form factor $F_D^0(s)$ corresponds to the infinite chains of the diagrams in Fig. 2 with the real D and $\bar{D}$ mesons in the intermediate states. The amplitude t_1^0 and the form factor f_D^0 specify the structure of primary mechanisms included in the model to describe the ψ'' resonance region. The constants λ and λ_γ effectively take into account background (nonresonant in the ψ'' region) contributions to the strong amplitude and form factor, respectively, and the constants $g_{\psi'' D\bar{D}}$ and $g_{\psi''\gamma}$ describe couplings of the ψ'' to the $D\bar{D}$ and virtual γ quantum, respectively. The unitarity requirement is fulfilled: The phase of the form factor $F_D^0(s)$ is defined by the phase of the amplitude $T_1^0(s)$. This phase has the dynamical origin. The physical content of Eqs. (5) and (6) will become more clear if they are rewritten in the form of Eqs. (2) and (3), respectively. As a result, we obtain the following expressions for the background and resonance components of $T_1^0(s)$:

$$T_{bg} = \frac{e^{2i\delta_{bg}(s)} - 1}{2i} = \frac{\nu(s)\lambda}{1 - i\nu(s)\lambda}\,, \quad T_{res} = \frac{\sqrt{s}\Gamma_{\psi'' D\bar{D}}(s)}{M^2_{\psi''} - s + \mathrm{Re}\Pi_{\psi''}(M^2_{\psi''}) - \Pi_{\psi''}(s)}\,, \tag{7}$$

$$\mathrm{Im}\Pi_{\psi''}(s) = \sqrt{s}\Gamma_{\psi'' D\bar{D}}(s) = \frac{g^2_{\psi'' D\bar{D}}(s)}{6\pi}\,\nu(s)\,, \quad \mathrm{Re}\Pi_{\psi''}(s) = -\lambda\frac{g^2_{\psi'' D\bar{D}}(s)}{6\pi}\,\nu(s)^2\,, \tag{8}$$

$$M^2_{\psi''} = m^2_{\psi''} - \mathrm{Re}\Pi_{\psi''}(M^2_{\psi''})\,, \quad g_{\psi'' D\bar{D}}(s) = g_{\psi'' D\bar{D}}/|1 - i\nu(s)\lambda|\,. \tag{9}$$

For the form factor we obtain

$$F_D^0(s) = e^{\delta_1^0(s)}\frac{(m^2_{\psi''} - s)\lambda_\gamma(s) + g_{\psi''\gamma} g_{\psi'' D\bar{D}}(s)}{|M^2_{\psi''} - s + \mathrm{Re}\Pi_{\psi''}(M^2_{\psi''}) - \Pi_{\psi''}(s)|}\,, \tag{10}$$

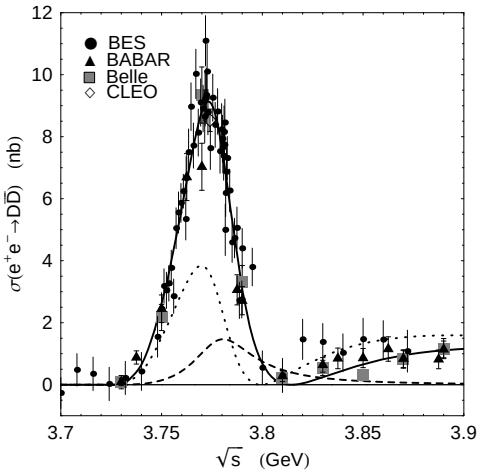

Figure 3: The resonance plus background model. The solid curve is the result of fitting the data with the use of Eqs. (4) and (10). The dashed curve shows the contribution from the ψ'' resonance production ($\sim g_{\psi''\gamma}$ in F_D^0), and the dotted curve shows the contribution from the background production ($\sim \lambda_\gamma$ in F_D^0) modified by the strong resonance and background final-state interactions.

where $\delta_1^0(s) = \delta_{bg}(s) + \delta_{res}(s)$; $\delta_{res}(s)$ is the phase of T_{res} and $\lambda_\gamma(s) = \lambda_\gamma/|1 - i\nu(s)\lambda|$.

Thus $F_D^0(s)$ incorporates the resonance contribution (proportional to $g_{\psi''\gamma}$) modified (dressed) by the strong background [21] and the proper background contribution (proportional to λ_γ) modified by the strong resonance and background final-state interactions. Because the numerator in Eq. (10) is proportional to the polynomial in s, $\lambda_\gamma(m_{\psi''}^2 - s) + g_{\psi''\gamma}g_{\psi''D\bar{D}}$, with real coefficients, the dip in $\sigma(e^+e^- \to D\bar{D})$ near 3.81 GeV can be explained by the zero in $F_D^0(s)$, caused by compensation between the ψ'' resonance and background contributions.

As is seen from Fig. 3, the constructed model for $F_D^0(s)$ yields the quite reasonable description of the data (here $\chi^2 \approx 123$, which is much better than the above χ^2 values for the fits shown in Fig. 1). For the solid curve in Fig. 3, the cross section at the maximum (located at $\sqrt{s} = \sqrt{s_{max}} \approx 3.773$ GeV) $\sigma_{max} \approx 9.13$ nb, the full width of the peak at its half maximum $\Gamma_{hmax} \approx 29.7$ MeV, and the effective electron width of the resonance structure $\Gamma_{e^+e^-}^{eff} = s_{max}\sigma_{max}\Gamma_{hmax}/(12\pi) \approx 0.263$ keV. These characteristics are in close agreement with those quoted by PDG [16] as the averaged individual characteristics of the ψ'' resonance. However, the peak (in its line shape there is a zero at $\sqrt{s} \approx 3.814\,\mathrm{GeV}$) does not correspond to a solitary resonance. Therefore, it is reasonable that the model parameters for ψ'' differ from the effective parameters of the visible peak. The curves in Fig. 3 correspond to the following values of the fitted parameters: $m_{\psi''} = 3.799$ GeV, $g_{\psi''D\bar{D}} = \pm 19.35$, $g_{\psi''\gamma} = \pm 0.1483$ GeV^2, $\lambda = -30.35$ GeV^{-2}, and $\lambda_\gamma = \pm 25.07$ [if $\lambda_\gamma > 0$ (< 0), then $g_{\psi''\gamma}g_{\psi''D\bar{D}} > 0$ (< 0), see Eq. (10)]. As the individual characteristics of the ψ'' resonance, one can take the quantities dressed (renormalized) by the background contributions [see Eqs. (7)–(9)]: $M_{\psi''} = 3.784$ GeV, $\Gamma_{\psi''D\bar{D}}^{ren} = \Gamma_{\psi''D\bar{D}}(M_{\psi''}^2)/Z_{\psi''} = 37.61$ MeV, and $\Gamma_{\psi''e^+e^-}^{ren} = \Gamma_{\psi''e^+e^-}/Z_{\psi''} = 0.05181$ keV, where $Z_{\psi''} = 1 + \mathrm{Re}\Pi'_{\psi''}(M_{\psi''}^2) = 1.748$ and $\Gamma_{\psi''e^+e^-} = 4\pi\alpha^2 g_{\psi''\gamma}^2/(3M_{\psi''}^3)$.

The obvious drawback of the considered model is the uncertain nature of the background contributions. However, the model can be easily improved. It is clear that the main sources of the background in the ψ'' region are the tails from the J/ψ, $\psi(2S)$, $\psi(4040)$, $\psi(4160)$ and other resonances. The right number of resonances can be incorporated in the model by adding the corresponding pole terms to expressions for $t_1^0(s)$ and $f_D^0(s)$. In that case, the parameters λ and λ_γ will effectively describe the contributions from the residual background, and it is hoped that they will be small. Below, we will consider in detail the model taking into account the $\psi(2S)$ resonance contribution and discuss additional ways of checking this model.

• **The model for F_D^0 with the ψ'' and $\psi(2S)$ resonances.** The connection of the

$\psi(2S)$ contribution does not change the structure of Eqs. (5) and (6) for T_1^0 and F_D^0. Only the functions t_1^0 and f_D^0 change. Now they are given by

$$t_1^0(s) = \lambda + \frac{1}{6\pi}\frac{g^2_{\psi(2S)D\bar{D}}}{m^2_{\psi(2S)} - s} + \frac{1}{6\pi}\frac{g^2_{\psi''D\bar{D}}}{m^2_{\psi''} - s}\,, \quad f_D^0(s) = \lambda_\gamma + \frac{g_{\psi(2S)\gamma}g_{\psi(2S)D\bar{D}}}{m^2_{\psi(2S)} - s} + \frac{g_{\psi''\gamma}g_{\psi''D\bar{D}}}{m^2_{\psi''} - s}\,. \quad (11)$$

Hereinafter $m_{\psi(2S)} = 3.6861$ GeV and $\Gamma_{\psi(2S)e^+e^-} = 2.35$ keV [16]; from the relation $\Gamma_{\psi(2S)e^+e^-} = 4\pi\alpha^2 g^2_{\psi(2S)\gamma}/(3m^3_{\psi(2S)})$, we get $g_{\psi(2S)\gamma} \approx \pm 0.7262$ GeV^2; $g_{\psi(2S)D\bar{D}}$ is a free parameter.

Owing to the common $D^0\bar{D}^0$ and D^+D^- coupled channels, the ψ'' and $\psi(2S)$ resonances can transform into each other (i.e., mix); for example, $\psi'' \to D\bar{D} \to \psi(2S)$. Therefore, it is very useful to rewrite Eqs. (5) and (6) for the amplitude T_1^0 and the form factor F_D^0 in terms which would reflect this physical aspect of the model and, in particular, introduce the amplitude describing the $\psi'' - \psi(2S)$ mixing.

Let us write the background amplitude in the form similar to Eq. (7)

$$T_{bg} = (e^{2i\delta_{bg}(s)} - 1)/(2i) = \nu(s)\lambda/(1 - i\nu(s)\lambda) \quad (12)$$

and represent T_{res}, corresponding to the complex of the mixed ψ'' and $\psi(2S)$ resonances, dressed by the residual background, in the following symmetric form [22, 23, 24]:

$$T_{res} = \frac{(m^2_{\psi''} - s)\mathrm{Im}\Pi_{\psi(2S)}(s) + (m_{\psi(2S)} - s)\mathrm{Im}\Pi_{\psi''}(s)}{D_{\psi''}(s)D_{\psi(2S)}(s) - \Pi^2_{\psi''\psi(2S)}(s)}\,, \quad (13)$$

where $D_{\psi''}(s)$ and $D_{\psi(2S)}(s)$ are the inverse propagators of ψ'' and $\psi(2S)$, respectively,

$$D_{\psi''}(s) = m^2_{\psi''} - s - \Pi_{\psi''}(s)\,, \quad D_{\psi(2S)}(s) = m^2_{\psi(2S)} - s - \Pi_{\psi(2S)}(s)\,, \quad (14)$$

$$\Pi_{\psi''}(s) = \frac{i}{6\pi}\frac{g^2_{\psi''D\bar{D}}}{1 - i\nu(s)\lambda}\,\nu(s)\,, \quad \Pi_{\psi(2S)}(s) = \frac{i}{6\pi}\frac{g^2_{\psi(2S)D\bar{D}}}{1 - i\nu(s)\lambda}\,\nu(s)\,, \quad (15)$$

and $\Pi_{\psi''\psi(2S)}(s)$ is the amplitude describing the $\psi'' - \psi(2S)$ mixing caused by the $\psi'' \to D\bar{D} \to \psi(2S)$ transitions via the real $D\bar{D}$ intermediate states,

$$\Pi_{\psi''\psi(2S)}(s) = \frac{i}{6\pi}\frac{g_{\psi''D\bar{D}}g_{\psi(2S)D\bar{D}}}{1 - i\nu(s)\lambda}\,\nu(s)\,. \quad (16)$$

For the form factor, we get

$$F_D^0(s) = \frac{e^{i\delta_{bg}(s)}\,\mathcal{R}_{D\bar{D}}(s)}{D_{\psi''}(s)D_{\psi(2S)}(s) - \Pi^2_{\psi''\psi(2S)}(s)} \quad (17)$$

where $\mathcal{R}_{D\bar{D}}(s) = (m^2_{\psi''} - s)(m^2_{\psi(2S)} - s)\lambda_\gamma(s) + (m^2_{\psi''} - s)g_{\psi(2S)\gamma}g_{\psi(2S)D\bar{D}}(s) + (m^2_{\psi(2S)} - s)g_{\psi''\gamma}g_{\psi''D\bar{D}}(s)$ and $g_{\psi(2S)D\bar{D}}(s) = g_{\psi(2S)D\bar{D}}/|1 - i\nu(s)\lambda|$.

The curves in Fig. 4 correspond to the following values of the fitted parameters: $m_{\psi''} = 3.784$ GeV, $g_{\psi''D\bar{D}} = \pm\,13.21$, $g_{\psi''\gamma} = \pm\,0.2237$ GeV^2, $g_{\psi(2S)D\bar{D}} = \pm\,12.91$, $\lambda = 26.89$ GeV^{-2}, and $\lambda_\gamma = \pm\,2.456$ [if $\lambda_\gamma > 0$ (< 0), then $g_{\psi''\gamma}g_{\psi''D\bar{D}} > 0$ (< 0) and $g_{\psi(2S)\gamma}g_{\psi(2S)D\bar{D}} < 0$ (> 0)]. Note that here $|\lambda_\gamma|$ is about an order of magnitude smaller than in the previous case, as qualitatively expected. For this fit, $\chi^2 \approx 125$. The form factor has the zero at $\sqrt{s} \approx 3.816$ GeV.

As the individual characteristics of the ψ'' resonance, one can take again the quantities dressed (renormalized) by the background contributions: $M_{\psi''} = 3.789$ GeV, $\Gamma^{ren}_{\psi''D\bar{D}} = \Gamma_{\psi''D\bar{D}}(M^2_{\psi''})/Z_{\psi''} = 58.03$ MeV, and $\Gamma^{ren}_{\psi''e^+e^-} = \Gamma_{\psi''e^+e^-}/Z_{\psi''} = 0.2973$ keV, where $Z_{\psi''} = 1 + \mathrm{Re}\Pi'_{\psi''}(M^2_{\psi''}) = 0.6905$ and $\Gamma_{\psi''e^+e^-} = 4\pi\alpha^2 g^2_{\psi''\gamma}/(3M^3_{\psi''})$. We calculated the above parameters with the use of Eqs. (7)–(9) by making the substitution $\lambda \to \lambda + \frac{1}{6\pi}\frac{g^2_{\psi(2S)D\bar{D}}}{m^2_{\psi(2S)} - s}$; i.e.,

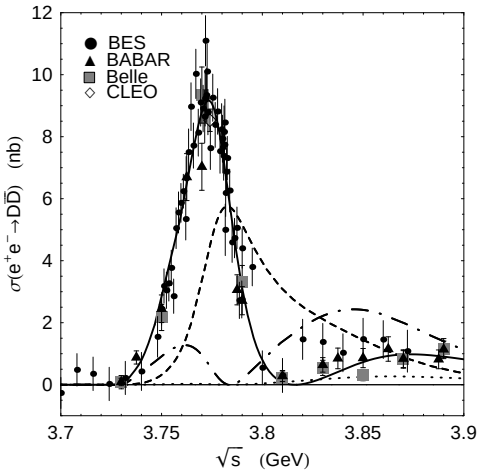

Figure 4: The model with the ψ'' and $\psi(2S)$ resonances. The solid curve is the fit using Eqs. (4) and (17). The dashed, dot-dashed, and dotted curves show the ψ'', $\psi(2S)$, and background production contributions proportional to the coupling constants $g_{\psi''\gamma}$, $g_{\psi(2S)\gamma}$, and λ_γ in $\mathcal{R}_{D\bar{D}}(s)$, respectively.

in the ψ'' region, we included in T_{bg} the total background from λ and $\psi(2S)$ and took into account in T_{res} the ψ'' contribution dressed by this total background.

Notice that the information only on the reactions $e^+e^- \to D\bar{D}$ is still lacking to give reliable conclusions about the separate components of the reaction amplitude. The performed analysis indicates that these components can be very different in the different models. On the other hand, it is clear that the interference pattern in the ψ'' region depends on the reaction. Therefore, to toughen the selection of the models one should compare their predictions with the experimental data on the mass spectra for several different reactions. For example, after the fitting of the $e^+e^- \to D\bar{D}$ data we all know about $D\bar{D}$ elastic scattering in the P-wave at the model level [in particular, $\sigma(D^0\bar{D}^0 \to D^0\bar{D}^0) = 3\pi|\sin\delta_1^0(s)|^2/p_0^2(s)$]. Unfortunately, these predictions are not possible to verify. However, there are many other reactions which can be measured.

4. The ψ'' shape in non-$D\bar{D}$ channels

Now we apply the last described model to construct the mass spectra in the reactions $e^+e^- \to \gamma\chi_{c0}$, $J/\psi\eta$, $\phi\eta$. In the ψ'' region, we restrict ourselves to the contributions only from the ψ'' and $\psi(2S)$ resonances, taking into account their couplings to the $\gamma\chi_{c0}$, $J/\psi\eta$, and $\phi\eta$ channels in the first order of perturbation theory. Thus the cross section for $e^+e^- \to ab$ ($ab = \gamma\chi_{c0}$, $J/\psi\eta$, $\phi\eta$) can be written as

$$\sigma^{ab}(s) = 4\pi\alpha^2 k_{ab}^3(s)\,|F_{ab}(s)|^2\,/(3s^{3/2})\,. \tag{18}$$

Here $k_{ab}(s) = \sqrt{[s-(m_a+m_b)^2][s-(m_a-m_b)^2]}\,/(2\sqrt{s})$ and the form factor

$$F_{ab}(s) = \frac{\mathcal{R}_{ab}(s)}{D_{\psi''}(s)D_{\psi(2S)}(s) - \Pi^2_{\psi''\psi(2S)}(s)}\,, \tag{19}$$

where $\mathcal{R}_{ab}(s) = g_{\psi(2S)\gamma}[D_{\psi''}(s)g_{\psi(2S)ab} + \Pi_{\psi''\psi(2S)}(s)g_{\psi''ab}] + g_{\psi''\gamma}[D_{\psi(2S)(s)}g_{\psi''ab} + \Pi_{\psi''\psi(2S)}(s) \times g_{\psi(2S)ab}]$; $g_{\psi(2S)ab}$, $g_{\psi''ab}$ are the coupling constants of the $\psi(2S)$, ψ'' to the ab channel.

We use the following information about the $\psi(2S)$ decays into $ab = \gamma\chi_{c0}$, $J/\psi\eta$, $\phi\eta$ [16, 25]: $B(\psi(2S) \to ab) = 9.68\%$, 3.28%, $(2.8^{+1.0}_{-0.8}) \times 10^{-5}$, $\Gamma_{\psi(2S)ab}$ (in keV) $= 29.4$, 10.0, $(8.5^{+3.0}_{-2.4}) \times 10^{-3}$, $g_{\psi(2S)ab}$ (in GeV^{-1}) $= \pm 0.25$, ± 0.22, $\pm(2.7^{+0.5}_{-0.4}) \times 10^{-4}$ (errors $< 10\%$ are not shown). The values of $g_{\psi(2S)ab}$ are obtained from the data on the $\psi(2S) \to ab$ decay widths by the formula $\Gamma_{\psi(2S)ab} = g^2_{\psi(2S)ab}k^3_{ab}(m^2_{\psi(2S)})/(12\pi)$.

Note that the available information about the $\psi'' \to \gamma\chi_{c0}$, $J/\psi\eta$, $\phi\eta$ decays are very poor [16]. The cross sections for $e^+e^- \to \gamma\chi_{c0}$, $J/\psi\eta$, $\phi\eta$ were measured by CLEO [25] at a single

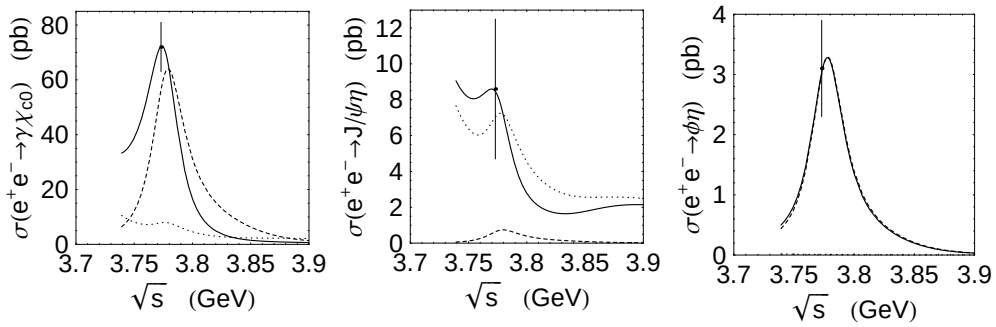

Figure 5: The cross sections for $e^+e^- \to \gamma\chi_{c0}$, $e^+e^- \to J/\psi\eta$, and $e^+e^- \to \phi\eta$.

point in energy $\sqrt{s} = 3773$ MeV. Their approximate values are presented in Fig. 5 by the dots with errors. They allow us to roughly estimate the coupling constants $g_{\psi''\gamma\chi_{c0}} \approx 0.54$ GeV^{-1}, $g_{\psi'' J/\psi\eta} \approx 0.053$ GeV^{-1}, and $g_{\psi''\phi\eta} \approx 1.12 \times 10^{-2}$ GeV^{-1}, by using Eqs. (18) and (19), to construct the corresponding cross sections. Here, as an illustration, we put $g_{\psi(2S)ab}$ and $g_{\psi'' ab} > 0$, and $g_{\psi(2S)\gamma}/g_{\psi''\gamma} < 0$. The solid curves in Fig. 5 show the $e^+e^- \to ab$ cross sections; the dashed and dotted curves show the ψ'' and $\psi(2S)$ contributions proportional to $[g_{\psi''\gamma}D_{\psi(2S)}(s) + g_{\psi(2S)\gamma}\Pi_{\psi''\psi(2S)}(s)]g_{\psi'' ab}$ and $[g_{\psi(2S)\gamma}D_{\psi''}(s) + g_{\psi''\gamma}\Pi_{\psi''\psi(2S)}(s)]g_{\psi(2S)ab}$ in $\mathcal{R}_{ab}(s)$, respectively. Note that the cross section for $e^+e^- \to \phi\eta$ is completely dominated by the ψ'' contribution. These examples tell us that the mass spectra in the ψ'' region in the non-$D\bar{D}$ channels can be very diverse. Therefore we should expect that the data on such spectra will impose severe restrictions on the constructed dynamical models.

5. On ambiguity of resonance parameters

Here we comment on the ambiguity of the interfering resonances parameters determination, which has been discussed in Refs. [11, 12, 17]. Let us write the $e^+e^- \to h\bar{h}$ amplitude involving the resonance and background contributions in the form [17]

$$F(E) = A_x e^{i\varphi_x}/(M - E - i\Gamma/2) + B_x \tag{20}$$

Here $E = \sqrt{s}$, M, Γ, A_x, φ_x, and B_x are the real parameters. At fixed M and Γ, there are two solutions for A_x, φ_x, and B_x: (I) $A_x = A$, $B_x = B$, $\varphi_x = \varphi$, (II) $A_x = \sqrt{A^2 - 2AB\Gamma\sin\varphi + B^2\Gamma^2}$, $B_x = B$, $\tan\varphi_x = -\tan\varphi + B\Gamma/(A\cos\varphi)$. They yield the same cross section as a function of energy, $\sigma(E) = |F(E)|^2$, and differ in the magnitude and phase of the resonance contribution [17]. For example, at $M = 3.77$ GeV, $\Gamma = 0.03$ GeV, $A = 0.045$ nb$^{1/2}$GeV, $\varphi = 0$, and $B = 1.5$ nb$^{1/2}$, solution (II) gives $A_x = \sqrt{2}A$ and $\varphi_x = \pi/4$. For each energy, the two solutions also give the different overall phase, $\delta = \delta_{res} + \delta_{bg}$, of the amplitude $F(E)$. For the above numerical example, the phase δ_{bg} corresponding to solutions (I) and (II) is shown in Fig. 6 by the dashed and solid curves, respectively; the phase $\delta_{res} = \arctan[\frac{\Gamma}{2(M-E)}]$ is shown by the dotted curve. The origin of the rapid change of the phase δ_{bg} (which is additional to δ_{res}) requires a special dynamical explanation (for example, the presence of extra intermediate states), for which we do not see at present any reasons.

6. Conclusion

• We tried to show that the shape of the ψ'' resonance keep important information about the production mechanism and interference with background. We have considered the models satisfying the unitarity requirement and obtained good descriptions of the current data on the $e^+e^- \to D\bar{D}$ reaction cross section, in particular, in the model with the mixed ψ'' and $\psi(2S)$ resonances. We have extracted from experiment $g^2_{\psi(2S)D\bar{D}}/(4\pi) \approx 13$.

• Further improvement of the data and matching the results from the different groups on the reactions $e^+e^- \to D\bar{D}$ can result in the crucial progress in understanding the complicate mechanism of the ψ'' resonance formation.

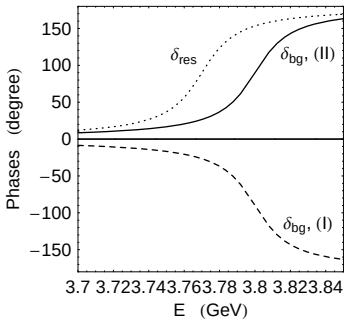

Figure 6: The ambiguity of the overall phase of the $e^+e^- \to h\bar{h}$ reaction amplitude defined in Eq. (20).

• As we have shown, the measurements of the mass spectra in the ψ'' region in the non-$D\bar{D}$ channels, such as $e^+e^- \to \gamma\chi_{c0}$, $J/\psi\eta$, $\phi\eta$, etc., will also contribute to a comprehensive study of the ψ'' resonance physics and the effective selection of theoretical models.

• Additional information about the ψ'' in the $D\bar{D}$ mass spectra can be extracted, for example, from weak decays $B \to \psi'' K$ and photoproduction reactions at high energies $\gamma A \to \psi'' A$.

This work was supported in part by RFBR, Grant No. 10-02-00016, and Interdisciplinary Project No. 102 of Siberian division of RAS.

References

[1] P.A. Rapidis *et al.*, Phys. Rev. Lett. **39**, 526 (1977), I. Peruzzi *et al.*, Phys. Rev. Lett. **39**, 1301 (1977).

[2] W. Bacino *et al.*, Phys. Rev. Lett. **40**, 671 (1978).

[3] R.H. Schindler, *et al.*, Phys. Rev. D **21**, 2716 (1980).

[4] M. Ablikim *et al.*, Phys. Lett. B **603**, 130 (2004); Phys. Rev. Lett. **97**, 121801 (2006); Phys. Lett. B **641**, 145 (2006).

[5] M. Ablikim *et al.*, Phys. Rev. Lett. **97**, 262001 (2006); Phys. Lett. B **652**, 238 (2007).

[6] M. Ablikim *et al.*, Phys. Lett. B **659**, 74 (2008); Phys. Lett. B **660**, 315 (2008); Phys. Rev. Lett. **101**, 102004 (2008); Phys. Lett. B **668**, 263 (2008).

[7] D. Besson *et al.*, Phys. Rev. Lett **96**, 092002 (2006); S. Dobbs *et al.*, Phys. Rev. D **76**, 112001 (2007); D. Besson *et al.*, Phys. Rev. Lett **104**, 159901(E) (2010).

[8] B. Aubert *et al.*, Phys. Rev. D **76**, 111105(R) (2007); Phys. Rev. D **79**, 092001 (2009).

[9] G. Pakhlova *et al.*, Phys. Rev. D **77**, 011103 (2008).

[10] V.V. Anashin *et al.*, Chinese Phys. C **34**, No.6, 650 (2010).

[11] K.Yu. Todyshev, Intrnational Workshop on e^+e^- collisions from Phi to Psi, 2011, BINP, Novosibirsk.

[12] V.V. Anashin *et al.*, Phys. Lett. B **711**, 292 (2012).

[13] H.-B. Li, X.-S. Qin, and M.-Z. Yang, Phys. Rev. D **81**, 011501 (2010).

[14] Y.-J. Zhang and Q. Zhao, Phys. Rev. D **81**, 034011 (2010).

[15] K. Nakamura *et al.* (Particle Data Group), J. Phys. G: Nucl. Part. Phys. **37**, 075021 (2010).

[16] J. Beringer *et al.* (Particle Data Group), Phys. Rev. D **86**, 010001 (2012).

[17] A.D. Bukin, arXiv:0710.5627.

[18] H. Mendez *et al.*, Phys. Rev. D **81**, 052013 (2010).

[19] H.-B. Li, in Proceedings of Hadron 2011; arXiv:1108.5789.

[20] N.N. Achasov, S.A. Devyanin, and G.N. Shestakov, Z. Phys. C **22**, 53 (1984).

[21] N.N. Achasov and G.N. Shestakov, Phys. Rev. D **49**, 5779 (1994).

[22] N.N. Achasov, S.A. Devyanin, and G.N. Shestakov, Phys. Lett. B **88**, 367 (1979).

[23] N.N. Achasov and G.N. Shestakov, Phys. Rev. D **58**, 054011 (1998).

[24] N.N. Achasov and A.A. Kozhevnikov, Phys. Rev. D **83**, 113005 (2011).

[25] R.A. Briere *et al.*, Phys. Rev. D **74**, 031106(R) (2006); N.E. Adam *et al.*, Phys. Rev. Lett. **96**, 082004 (2006); G.S. Adams *et al.*, Phys. Rev. D **73**, 012002 (2006).